

Hard QCD and Structure Functions

Rik Yoshida*

*Argonne National Laboratory
Argonne, IL. 60439 USA
E-mail: rik.yoshida@anl.gov*

ABSTRACT: Recent progress in experimental studies of perturbative Quantum Chromodynamics is reviewed.

1. Introduction

Quantum Chromodynamics (QCD), the strong interaction part of the Standard Model (SM), is a simple and elegant theory of the interaction of quarks and gluons. But because of the nature of the theory, whose coupling increases with distance, we do not yet fully understand how the measurements, made on hadrons, are described by QCD. The topic of this review is “hard” QCD where the experiments access interactions at scales which should be sufficiently high to apply perturbative QCD (pQCD). We must remember, however, that even at these high scales, the coupling constants are still relatively large, and higher order (HO) QCD calculations are usually important. In addition, we must guess, by means of models, the processes by which quarks and gluons become hadrons (hadronization). These considerations make experimental studies of QCD rather complicated in practice. In particular, in the assignment of theoretical uncertainties authors tend to choose different conventions. When looking at a particular measurement, it is important to ask what is being meant by the uncertainty being quoted before it can be compared to other measurements.

2. QCD at e^+e^-

In many ways, it is simplest to start the discussion with QCD studies at e^+e^- colliders, where there are no hadrons in the initial state. The observable to be measured by the experiment must be infra-red safe, i.e. invariant under a soft collinear QCD radiation. Typical examples for e^+e^- collisions are “event shapes”, where the momenta of all final state hadrons are combined in a way which is stable under $\vec{p}_i \rightarrow \vec{p}_k + \vec{p}_l$.

*Speaker.

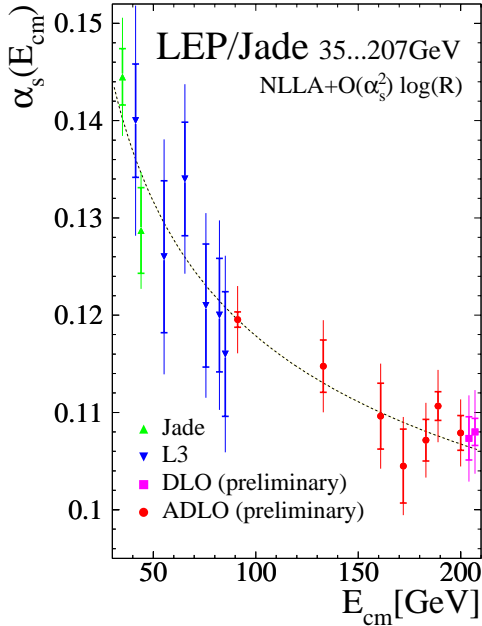


Figure 1: The strong coupling constant α_s determined from eventshape analyses in e^+e^- experiments.

“hadronized”. This is accomplished by Monte Carlo models[4]. While the hadronization models are tuned with data, there are no rigorous justification for their correctness.

2.1 Event shapes

In the present conference, the results from the highest energy runs at LEP II has been reported. As an example of an analysis that span a large range of e^+e^- cms energies, the strong coupling constant, α_s , determined from the event shapes at LEP and the Jade experiment at PETRA is shown in Figure 1 [5]. The running of α_s is convincingly demonstrated. The QCD predictions, in this case, are made with NLO fixed order calculations matched to a (next-to) leading log resummation. The strong coupling constant α_s is determined to 6%.

To match theory with the measurements, Monte Carlo hadronization models are used, which is usually not small in case of event shape variables. We will return to these corrections later in the talk.

2.2 Running b mass

A new measurement of the b quark mass at the LEP energies have been reported [6] by the OPAL collaboration. This result is based on measurements of the rates of tagged $b(\bar{b})$ events with three jets compared to those of the light quarks. Figure 2 shows the measurements together with earlier measurements from other LEP experiments and that

The QCD predictions which are used in the analyses of experimental data are composed of several components. For an observable, R , being measured in an experiment, a fixed-order (FO) pQCD calculation is made. These calculations need to be at least one order (next-to-leading NLO) beyond the “trivial” level for that observable. These fixed order calculations are usually supplemented by a partial accounting of the terms which are orders higher than that in the FO calculations. In some cases, where the observable R is small, it is possible to sum all terms of the type $\alpha_s^n \ln(1/R)^{n+1}$. This procedure is called leading log resummation. In other cases, Monte Carlo implementations of higher order radiation is used. These are usually either based on the parton shower model as in programs PYTHIA [1] and HERWIG [2], or on the color dipole model as in the program ARIADNE [3].

When the momenta of the partons approach the QCD confinement scale, they need to be

from SLD. Taken together with b mass measurements at the production threshold, the data demonstrates the running of b mass predicted by QCD.

2.3 QCD color factors

QCD color factors are a fundamental property of the theory. These factors are associated with particular vertices that couple quarks and gluons. Recalling the spins of quarks and gluons, it is not surprising that measurements of angular correlation of 4-jet events are sensitive to the color factors. In these measurements α_s is left as a free parameter to be determined. The α_s thus determined is consistent with those of other measurements but with an uncertainty of about 15%. Figure 3 shows the color factors determined from 4-jet final states at the Z resonance in a new analysis by ALEPH compared to the previous OPAL study [7]. This and other measurements of color factors show that they are consistent with the SU3 symmetry of QCD.

2.4 Summary: e^+e^-

All LEP experiments have reported updated results of QCD studies at the highest LEP II energies. There are several studies that cover 20–200 GeV CMS energies, and convincingly demonstrate the running of α_s . Errors on α_s determination is typically 3-5%, and all studies obtain consistent results. Running of the b mass has also been seen, and the basic check of QCD color factors give results that confirm the SU3 symmetry of the underlying theory.

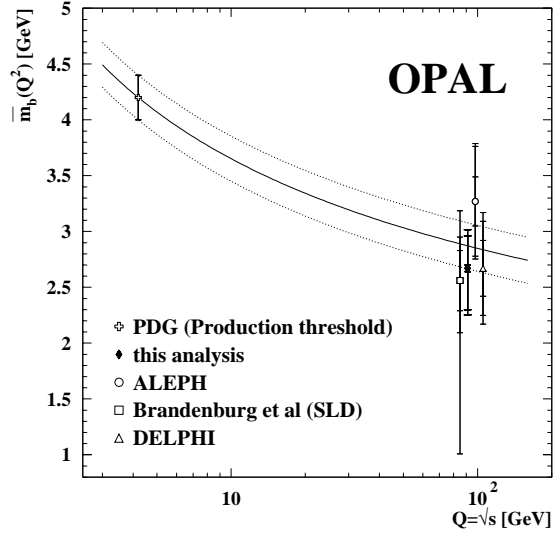


Figure 2: The mass of the b quark, determined at e^+e^- colliders compared to that from the production threshold measurements.

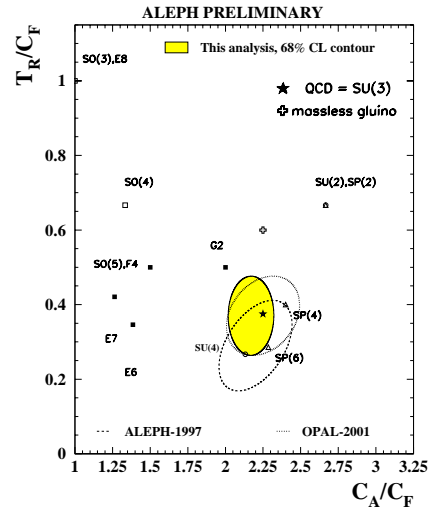


Figure 3: QCD color factors T_R , C_F , and C_A measured by OPAL and ALEPH experiments. Predictions of various different symmetry structures are indicated.

3. Structure Functions and Parton Distributions

3.1 Structure functions at HERA

Deep Inelastic Scattering (DIS) of electrons (or positrons) with a proton proceeds through the exchange of a virtual boson. The reaction can be described completely by two kinematic variables chosen to be the four-momentum transfer squared (or the virtuality of the exchanged boson), $Q^2 = -q^2$, and the Bjorken variable, x . In the Quark Parton Model, x is the fraction of the initial proton momentum carried by the struck parton. At the HERA ep collider, with \sqrt{s} of about 300 GeV, x and Q^2 can be varied over six orders of magnitude.

The DIS cross-section factorizes into a short-distance partonic cross-section, $\hat{\sigma}$, that can be calculated perturbatively in QCD, and a long-distance non-perturbative part, the parton densities, f .

At sufficiently high Q^2 , the parton densities, f , obey the DGLAP equation [8], which can be written schematically as:

$$\frac{\partial f}{\partial \ln Q^2} \sim f \otimes P, \quad (3.1)$$

where P are the splitting functions that describe the branching of quarks and gluons, and \otimes symbolizes a convolution.

The neutral current DIS differential cross-section can be written in terms of the proton structure functions F_i as

$$\frac{d\sigma^2}{dx dQ^2} = \frac{2\pi\alpha^2}{xQ^4} (Y_+ F_2 - y^2 F_L \mp Y_- x F_3), \quad Y_{\pm} = (1 \pm (1-y)^2) \quad (3.2)$$

where $y = Q^2/xs$ is the inelasticity parameter, and s is the CMS energy squared of the ep collision. For the HERA studies of the longitudinal structure function F_L , which is damped by y^2 and F_3 which arises from Z^0 exchange, the reader is referred to individual contributions [10, 11].

The structure function F_2 dominates the cross section in the largest part of the HERA kinematic range. At leading order,

$$F_2(x, Q^2) = x \sum_q e_q^2 (q(x, Q^2) + \bar{q}(x, Q^2)), \quad (3.3)$$

where q is the quark and \bar{q} the antiquark density distributions.

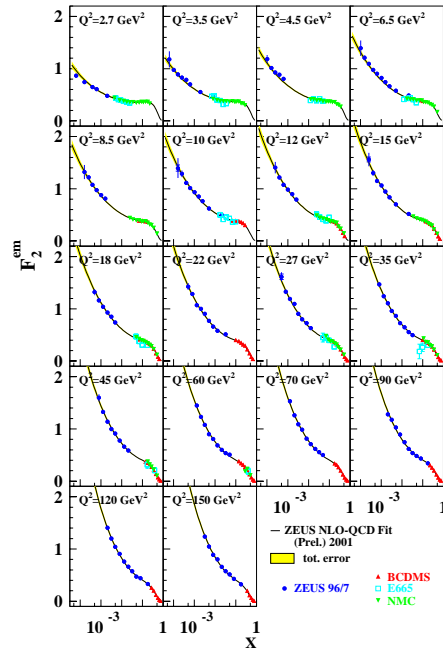


Figure 4: The measurement of F_2 by the ZEUS collaboration shown with the fixed target results and a NLO QCD fit. Similar data exists from the H1 collaboration.

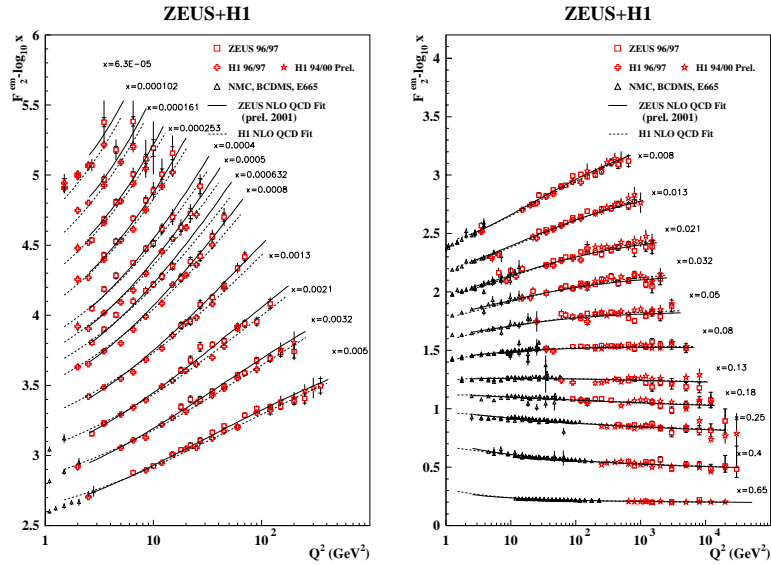


Figure 5: The most recent measurements of the structure function F_2 at HERA, shown together with fixed target experiment results. The lines are NLO QCD fits.

The latest measurements of F_2 at HERA [10] (Figure 4) confirm the steep rise of the structure function at small x with improved precision. The scaling violations (i.e. the Q^2 dependence of F_2 at fixed x) as shown in Figure 5. The logarithmic slope of F_2 at low x , in Leading Order (LO) DGLAP, is simply proportional to the gluon density of the proton times α_s [9].

In NLO DGLAP, the simple relationship of gluons to F_2 at LO no longer holds. However, the gluon density, and α_s may be extracted via NLO DGLAP fits to F_2 . The current determination of gluons are at $\approx \pm 10\%$ precision at $Q^2 = 5 \text{ GeV}$ and $x = 10^{-3}$. The coupling constant α_s is determined to 4-5%. The present errors are dominated by theory uncertainties.

New measurements of DIS cross sections at highest Q^2 using 100 pb^{-1} of e^+p data and 15 pb^{-1} of e^-p data have become available [11]. Figure 6 shows the HERA data at the highest Q^2 for both e^+ and e^- as well as for charged and neutral current interactions. The charged and neutral current cross-section approach each other at high Q^2 showing the unification of electromagnetic and weak forces. The data are well described by SM using the CTEQ5D parton distributions [12]. While this data is still not precise enough either for detailed studies of electroweak physics or parton distributions at high x , the luminosity upgrade at HERA which promises to increase the data 10 fold in 5-6 years, and provide longitudinally polarized e^\pm beams will open up new areas of study.

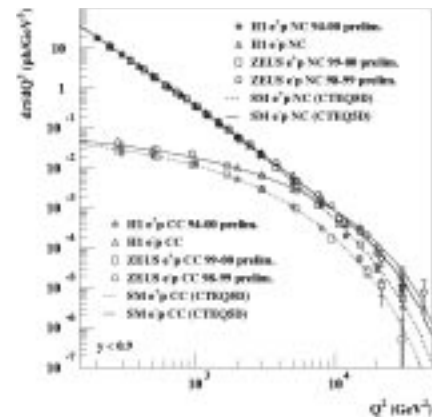


Figure 6: Charge current (CC) and neutral current (NC) cross sections for e^+ and e^- measured at HERA.

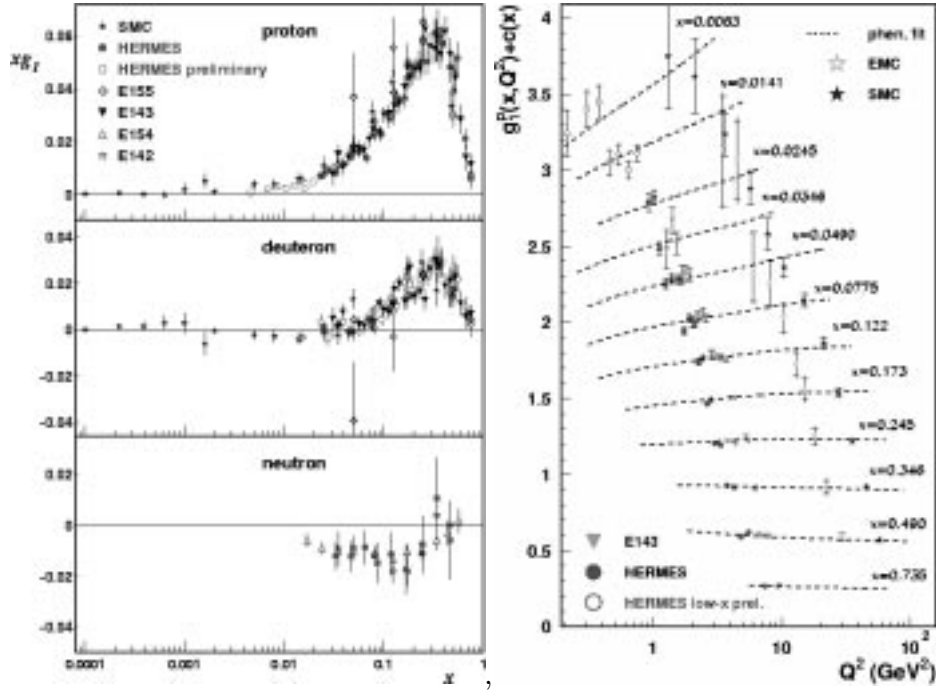


Figure 7: The world data on the spin structure function g_1 as function of x (left) and Q^2 (right).

3.2 Spin structure of the proton

The measurements of asymmetry in polarized lepton-nucleon scattering gives the spin structure function g_1 which, LO, is:

$$g_1(x) = \frac{1}{2} \sum_{i=1}^{n_f} e_i^2 [\Delta q_i(x) + \Delta \bar{q}_i(x)] \quad (3.4)$$

where Δq_i is the spin carried by the quark i . The world data on g_1 is shown on Figure 7 [13]. The scaling violation of g_1 is related in similar way to that of F_2 to the spin component carried by the gluon, which is thought to carry the “missing” spin of the proton, i.e. that not carried by the valence quarks. In principle, NLO QCD analyses of the same type performed on the spin averaged structure functions can determine the spin carried by the partons. This type of analyses in NLO, performed by two groups, were presented [14] in this conference. Figure 8 shows the results of one of the analyses [15]. The spin carried by the gluon is labeled $x\Delta G$. As can be seen the precision of this data is not yet at a point where a definitive statement on gluon spin can be made. The strong coupling constant α_s can also be extracted from these fits, and has an uncertainty of about 6%.

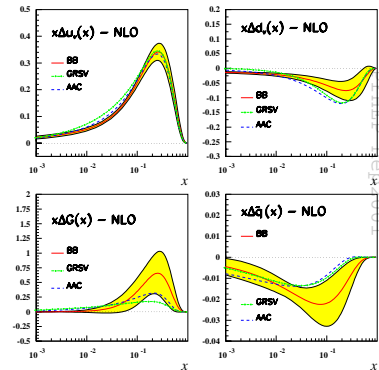
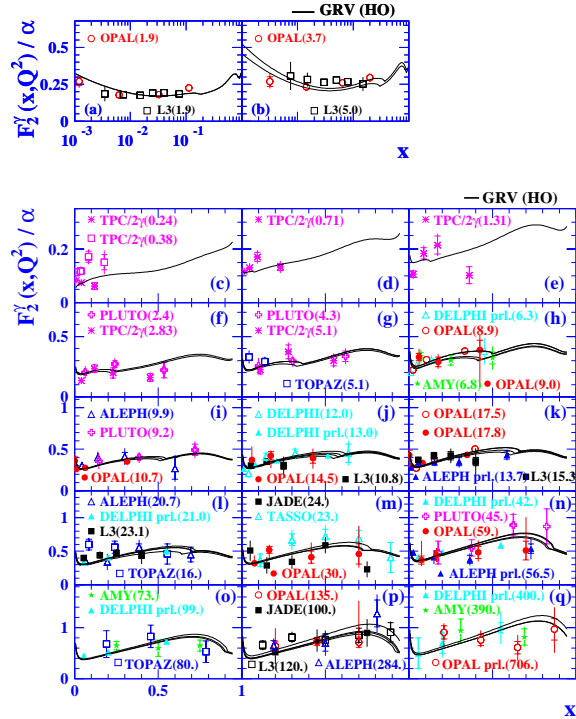


Figure 8: The results of a NLO QCD fit to polarized lepton data.

3.3 DIS of the photon

At e^+e^- machines, the structure of the photon may be measured by tagging either the positron or electron to measure the Q^2 of the virtual photon that probe the real photon emitted by the untagged beam lepton. This is a difficult measurement since a large part of the final state is lost down the beampipe. In this conference, OPAL reported new measurements of the photon structure function at low x and high Q^2 [16]. Figure 9 shows the of the world data on the photon structure function F_2^γ . The measurements do not yet extend to low enough x to determine if a rise similar to the proton F_2 is present in the photon.



3.4 Summary: structure functions and parton distributions

The electron-proton DIS data from HERA now spans six orders of magnitude in x and Q^2 . The experimental precision reached is about 3%. This data allows a precise determination of the gluon density in the proton at low x . The strong coupling constant has been determined to 4-5% from the scaling violations of F_2 . The uncertainty is now dominated by the theoretical uncertainties. The NNLO calculations are almost ready for application, and are expected to improve the precision of these measurements in the near future [18].

In parallel, there is now a strong effort from many groups to produce PDF's with correlated errors [17]. Some of these efforts also extend to polarized structure function.

Finally, some new data on photon structure has become available from OPAL.

Figure 9: The world's data on the photon structure function F_2^γ . The new measurements from OPAL are shown in (a), (b), and (q).

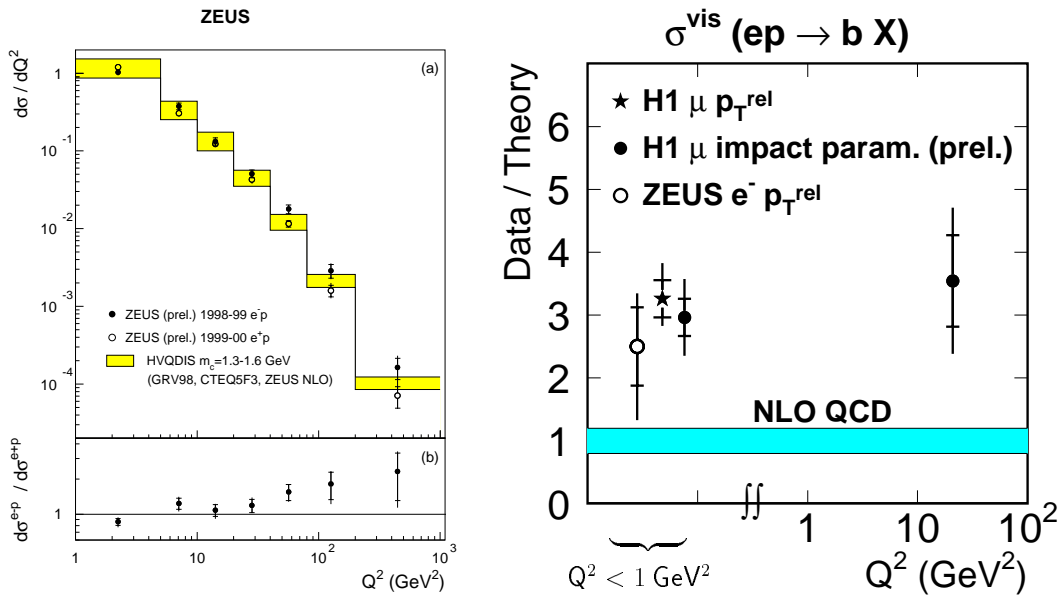


Figure 10: Heavy flavor production cross section at HERA. The charm production cross section (left) measurements from ZEUS, and the beauty production cross section (right), divided by the theoretical prediction, from H1 and ZEUS.

4. Hadrons in the initial state

4.1 Heavy flavor production in DIS

The parton distributions extracted from procedures described in the previous section can be used in QCD studies where there are hadrons in the initial state of the reaction. These studies are similar to those discussed in the section on e^+e^- collisions, but have the additional complication of a hadron whose partonic content is described by its PDF.

The goals of these analyses depend on the uncertainties associated with each piece of information that goes into the NLO QCD predictions for the process being studied. In cases where the PDF's are sufficiently well-known, the pQCD predictions are tested, and QCD parameters extracted in a way similar to the studies of e^+e^- collisions. In other cases, where the PDF's are not well-known, these studies can constrain or determine the PDF's.

Figure 10 (left) shows the measurement of the charm cross-section in ep collisions at the highest Q^2 accessible at HERA [19]. The measurements are in reasonable agreement with the QCD predictions using existing proton PDF's. The large uncertainty due to the uncertainty in the mass of charm quarks, however, limits the usefulness of this measurements as a constraint for the proton PDF's. Intriguingly, a difference in the e^+ and e^- cross-sections, that apparently increases with Q^2 , is observed at a 3σ level.

Figure 10 (right) shows the compilation of beauty production data from HERA [19], including the new measurement at high Q^2 by the H1 collaboration. The QCD predictions are consistently lower than and incompatible with the data, even when theoretical uncertainties are taken into account. This is surprising since the heavier b quark mass should

make the QCD prediction more reliable than in the case of charm. The b production cross-section in other processes will be discussed below.

4.2 Jet production in DIS

At high Q^2 at HERA, dijet productions proceeds predominantly via the QCD Compton process, which does not involve the gluon in the proton. Since the quark density of the proton is well-known, in contrast to the gluon density at high x , it is possible to use this data for a precise test of QCD.

Figure 11 compares the DIS total and dijet cross-section from ZEUS [20] with the QCD predictions. Taking the ratio of the two cross sections further reduces the sensitivity of the results to the proton PDF's. The strong coupling constant α_s is determined from this data to about 4%. Similar results are obtained by the H1 collaboration using the measurement of inclusive jet cross sections. It is notable that the theoretical uncertainties are comparable or larger than the experimental ones in these measurements.

The H1 collaboration has recently measured the 3-jet production cross-section 3-jet production for in DIS as well as the 3-jet to 2-jet rate [20]. A recent calculation [21] shows that the 3-jet to 2-jet ratio is particularly robust with small theoretical uncertainties. At the moment, the measurements are statistically limited, but with the advent of HERA II the situation will improve in the next few years.

4.3 Jets at the Tevatron

The description of the jet production at the Tevatron depends critically on the high x gluon distribution in the colliding proton and anti-proton. The early reports of excess above the QCD predictions at high E_t are now found to be compatible within the uncertainties of the gluon density at high x .

At this conference, the D0 collaboration has reported [22] on studies that extend the jet studies to higher rapidities, which correspond to lower values of x . Altogether, the Tevatron jet data now probe in the x range of ≈ 1 to 0.001. The results are compatible with the QCD predictions using the currently available proton PDF's.

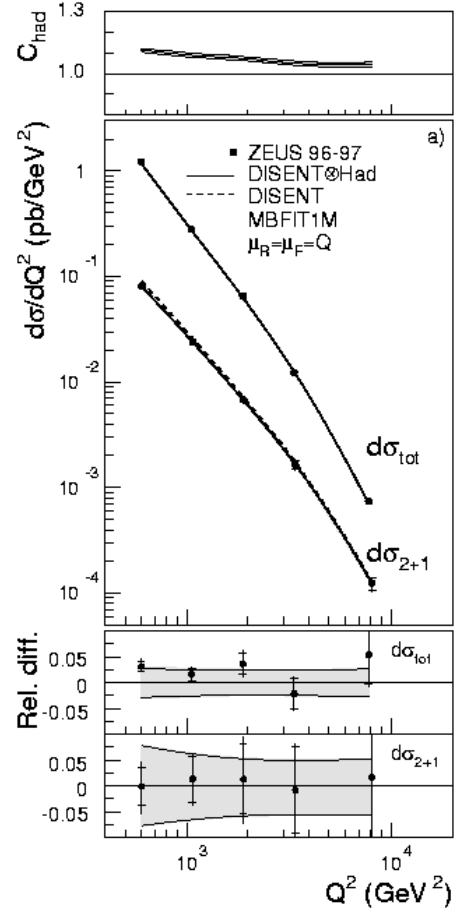


Figure 11: The measurement of total and dijet neutral current cross section from ZEUS. The measurements are compared to the standard model prediction. The hadronization correction is indicated at the top (C_{had})

4.4 Photon collisions at LEP

At LEP, photons which are emitted by the electron, or positron, beams correspond to the initial hadron in the present discussion. At LO, the photon couples directly to the hard process that produce the final states that is being studied, or be “resolved” into partons, one of which take part in the hard process. The variable x_γ is 1 in the former case and less than 1 for the latter. Figure 12 shows the preliminary measurement of dijets as a function of x_γ in photon-photon collisions at OPAL [23].

Since there are 2 photons, each event enters twice in this figure. The NLO QCD predictions do not contain hadronization corrections which accounts for some of the differences with the data. However, at low x_γ , the prediction is considerably lower than the data. This suggests that the photon PDF’s which are much less well-known than the proton one, are inadequate.

The charm production production cross section in photon-photon collisions have been measured upto the LEP II energies [24]. Within the large uncertainty in the prediction which comes from the uncertainty in the charm mass, the QCD calculations describe the data. This is not the case for b production, however [24].

The measurements of Figure 13 from, OPAL and L3 collaborations, show that the QCD prediction falls well below the data. Taken together with the ep data discussed above and that from the Tevatron reported in previous years indicate that QCD calculation of b production consistently falls below the measurements.

4.5 Photoproduction dijets at HERA

At HERA, the photon emitted by the electron (or positron) can, together with the proton, be considered as an initial state hadron. In this case, since the proton PDF’s are relatively well-known, the proton can considered to “probe” the photon. Figures 14 and 15 shows the measurements of the dijet photoproduction at HERA from ZEUS and H1 collaborations respectively [25]. The cuts on the jet energies are “asymmetric”, i.e. the two jets have different energy cuts. This is needed because NLO calculations are not reliable when the jets are both at the same minimum energy. In case of the ZEUS data, the minimum energy is 11 GeV, H1, 15

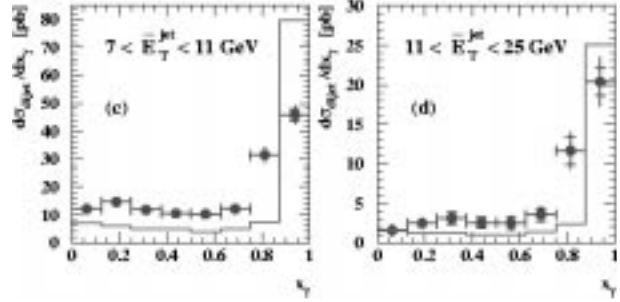


Figure 12: Dijet cross section for $\gamma\gamma$ collisions measurement from OPAL.

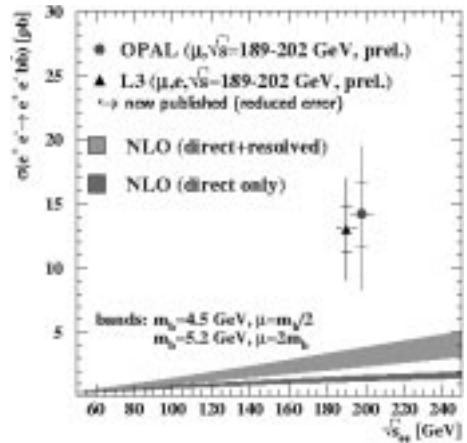


Figure 13: The b production cross section in $\gamma\gamma$ collisions measured by OPAL and L3.

GeV. In the case of H1, the QCD calculations agree with the data whereas for ZEUS the calculations are below the data. The source of this apparent discrepancy remainst to be clarified.

4.6 Summary: hadrons in the initial state

The determination of α_s from jet measurements at HERA have achieved uncertainties at the level of 4%. The uncertainties are dominated by theory, and higher order calculations are needed.

The Tevatron jet measurements have been extended to lower values of Bjorken x . The D0 collaboration finds good agreement with existing PDF's in this new kinematic region. The first Tevatron jet measurements using the k_T algorithm were presented by the D0 collaboration [22].

Some questions are emerging in the measurements that are sensitive to the photon PDF's. ZEUS and OPAL measurements find that the existing photon PDFs are not adequate to describe their dijet data. The H1 collaboration, on the other hand, finds the GRV-HO photon PDF [26] describes their dijet data well.

The QCD predictions of beauty cross-sections [27] are too low in photon-photon, proton-photon, and proton-anti-proton collisions.

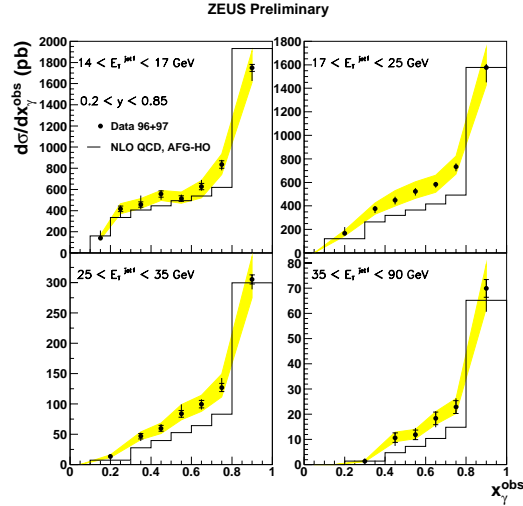


Figure 14: The dijet photoproduction cross section from ZEUS. The E_T values indicated are for one of the jets. The other jet has E_{Tmin} value of 11 GeV.

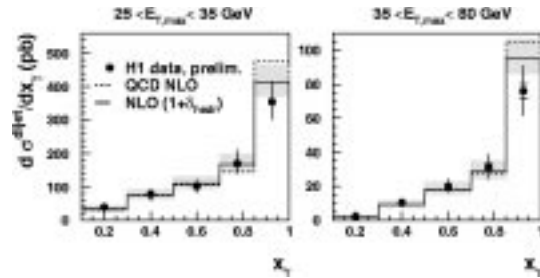


Figure 15: The dijet photoproduction cross section from H1. The E_T values indicated are for one of the jets. The other jet has E_{Tmin} value of 15 GeV.

5. Power corrections and event shapes

Beginning in the early 90's, a method of determining non-perturbative corrections which is independent of Monte Carlo models has been advocated. Briefly, the idea is to relate a particular type of divergence encountered in the QCD fixed order calculations to the non-perturbative corrections that are needed to ultimately cancel them. These divergences are called “renormalons”, and the resulting corrections are called “power corrections”. According to some authors power corrections [28], in case of structure functions are related to higher twist terms encountered in the Operator Product Expansion.

Power corrections only predict the form of the corrections and not the magnitude. Accordingly, in analyses using power corrections,

the form of the power corrections are used in a fit that include parameters that control the magnitude of the corrections.

Event shapes are the most common observables used in analyses involving power corrections, since the non-perturbative corrections are relatively large. Figure 16 shows (one minus) the average Thrust measured in e^+e^- collisions compared to NLO QCD theory (dotted line) and the prediction including non-perturbative corrections (solid line). Dokshitzer and Webber [29] have further postulated a universal parameter α_0 which controls the power corrections and are independent of the type of event shape observable.

Figure 17 shows an analysis made by Movilla-Fernandez et al. [5] of event shapes using power corrections of the Dokshitzer-Webber type, that span the energy range 14-189 GeV. The QCD calculations with the power corrections give a remarkably good description of the data over the very wide kinematic range. The authors have compared the power corrections with the non-perturbative corrections derived from Monte Carlo models. The two kinds of corrections can be rather similar as in the case of Thrust,

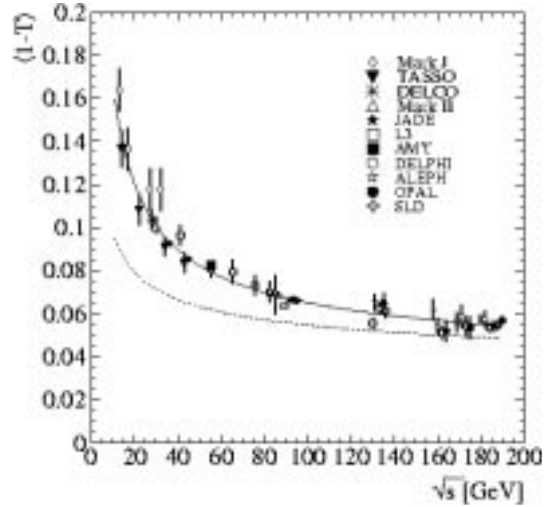


Figure 16: Average Thrust for e^+e^- collider events as a function of the cms energy

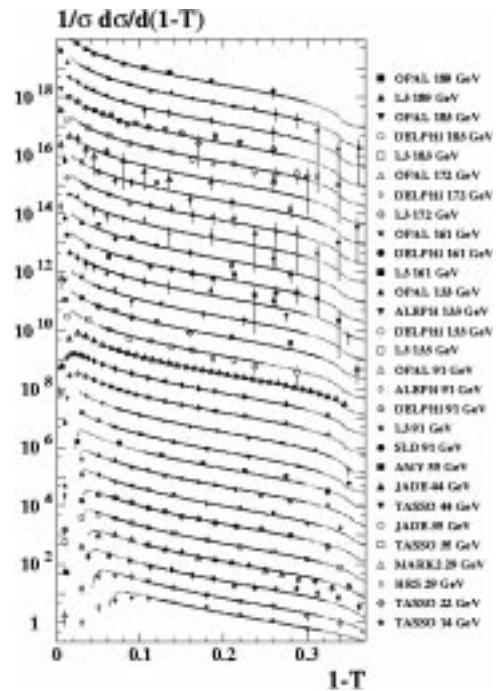


Figure 17: The differential Thrust distributions from e^+e^- data fitted with NLO QCD and power corrections.

but can also differ substantially in the case of Wide Jet Broadening, B_W (Figure 18). The results of the fits which determine α_0 and α_s simultaneously are largely consistent among different shape variables, and give remarkably small errors.

The DELPHI collaboration has performed a power correction analysis on their data using the “renormalization group independent” (RGI) scheme [5]. This is a method related to scale optimization scheme such as that of effective charge (ECH) [30]. When the RGI scheme is used in their analysis, it is found that the power correction terms become very small and are compatible with zero. While it is known that power corrections are not independent of the order to which the fixed order calculations are made, the significance of the success of RGI scheme is not clear at present.

The errors of the α_s determination from event shape analyses using power corrections are at the level of 2.5%, and are among the smallest of such measurements. The theoretical uncertainty of these measurements are subject to further clarification.

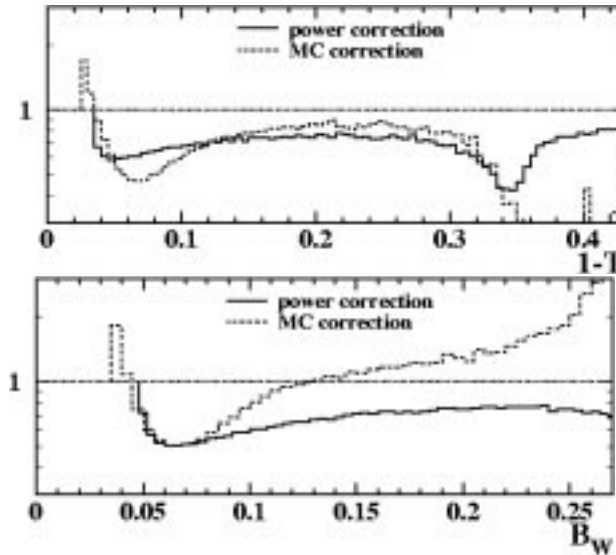


Figure 18: The non-perturbative corrections as determined by Monte Carlo compared to those obtained from power corrections. Top plot is the results for Thrust, whereas the bottom plot is that for Wide Jet Broadening.

6. Summary

The experimental study of QCD is still a vibrant and exciting field. Due to lack of time, I have had to leave out many interesting and important developments; the reader is referred to the individual contributions to these proceedings. There are now very many *precision* tests of QCD. A benchmark is the number of 3-6% determination of α_s reported here. Still, QCD is a complex topic. In many analyses, one needs to look at the “fine print”; it is not a simple matter of “who’s quoting the smallest errors”.

While on the whole, there is an impressively consistent picture, there are many questions in detail. Two years ago, one of the reviewers at this conference remarked upon the need for improvements in the theory. I was not able to cover this in detail but these improvements are now beginning to appear.

Finally, some of the most intriguing results in QCD are in the studies that involve boundaries of hard and soft QCD. While it is still far from achieving an understanding of the relationship between hadronic physics and QCD, many new results and phenomenology is leading to a renewed activity. The reader is referred to the proceeding in the soft-QCD session.

Acknowledgments

Review talks such as this cannot be written without help from many people. I would like to thank, in particular, A. Arneodo, I. Bertram, F. Chlebana, M. Dasgupta, A. Doyle, D. Elvira, B. Foster, G. Iacobucci, R. Nisius, P. Schleper, S. Soldner-Rembold, M. Vincet, J. Vossebeld, M. Wing and J. Whitmore. M. Derrick was kind enough to go through the manuscript. Any remaining mistakes, and misunderstandings are, of course, my own.

It is a pleasure to thank the organizers at Budapest. I am thankful, particularly, to the technical staff who, with great patience, helped me to make last minute revisions in the talk.

References

- [1] T. Sjöstrand, *Comput. Phys. Commun.* **82** (1994) 74.
- [2] G. Marchesini *et al.*, *Comput. Phys. Commun.* **67** (1992) 465.
- [3] L. Lönnblad, *Comput. Phys. Commun.* **71** (1992) 15.
- [4] B. R. Webber, *Nucl. Phys.* **B 238** (1984) 492;
B. Andersson *et al.*, *Phys. Rept.* **97** (1983) 31.
- [5] D. Wicke in Proceedings of the EPS International Conference on High Energy Physics, Budapest, 2001 (D. Horvath, P. Levai, A. Patkos, eds.), JHEP (<http://jhep.sissa.it/>) Proceedings Section, PrHEP-hep2001/001 and references therein.
- [6] P. Bambade in Proceedings of the EPS International Conference on High Energy Physics, Budapest, 2001 (D. Horvath, P. Levai, A. Patkos, eds.), JHEP (<http://jhep.sissa.it/>) Proceedings Section, PrHEP-hep2001/005 and references therein.

- [7] J. Vossebeld in Proceedings of the EPS International Conference on High Energy Physics, Budapest, 2001 (D. Horvath, P. Levai, A. Patkos, eds.), JHEP (<http://jhep.sissa.it/>) Proceedings Section, PrHEP-hep2001/003 and references therein.
- [8] L. N. Lipatov, *Sov. J. Nucl. Phys.* **20** (1975) 94;
V. N. Gribov and L. N. Lipatov, *Sov. J. Nucl. Phys.* **15** (1972) 438;
G. Altarelli and G. Parisi, *Nucl. Phys.* **B 129** (1977) 298;
Y. L. Dokshitzer, *Sov. Phys. JETP* **46** (1977) 641.
- [9] K. Prytz, *Phys. Lett.* **B 311** (1993) 286.
- [10] A. Cooper-Sarkar in Proceedings of the EPS International Conference on High Energy Physics, Budapest, 2001 (D. Horvath, P. Levai, A. Patkos, eds.), JHEP (<http://jhep.sissa.it/>) Proceedings Section, PrHEP-hep2001/009 and references therein;
R. Wallny in Proceedings of the EPS International Conference on High Energy Physics, Budapest, 2001 (D. Horvath, P. Levai, A. Patkos, eds.), JHEP (<http://jhep.sissa.it/>) Proceedings Section, PrHEP-hep2001/008 and references therein.
- [11] E. Rizvi in Proceedings of the EPS International Conference on High Energy Physics, Budapest, 2001 (D. Horvath, P. Levai, A. Patkos, eds.), JHEP (<http://jhep.sissa.it/>) Proceedings Section, PrHEP-hep2001/007 and references therein.
- [12] H. L. Lai *et al.*, *Phys. Rev.* **D 55** (1997) 1280.
- [13] J. Stewart in Proceedings of the EPS International Conference on High Energy Physics, Budapest, 2001 (D. Horvath, P. Levai, A. Patkos, eds.), JHEP (<http://jhep.sissa.it/>) Proceedings Section, PrHEP-hep2001/011 and references therein.
- [14] A. Sidorov in Proceedings of the EPS International Conference on High Energy Physics, Budapest, 2001 (D. Horvath, P. Levai, A. Patkos, eds.), JHEP (<http://jhep.sissa.it/>) Proceedings Section, PrHEP-hep2001/012 and references therein.
- [15] J. Blümlein and H. Boettcher, Abs. 165, HEP2001, Budapest.
- [16] Á. Csilling in Proceedings of the EPS International Conference on High Energy Physics, Budapest, 2001 (D. Horvath, P. Levai, A. Patkos, eds.), JHEP (<http://jhep.sissa.it/>) Proceedings Section, PrHEP-hep2001/013 and references therein.
- [17] M. Botje, *Eur. Phys. J.* **C 14** (2000) 285.
J. Pumplin, D. R. Stump and W. K. Tung, hep-ph0008191.
- [18] S. Moch in Proceedings of the EPS International Conference on High Energy Physics, Budapest, 2001 (D. Horvath, P. Levai, A. Patkos, eds.), JHEP (<http://jhep.sissa.it/>) Proceedings Section, PrHEP-hep2001/010 and references therein.
- [19] F. Sefkow in Proceedings of the EPS International Conference on High Energy Physics, Budapest, 2001 (D. Horvath, P. Levai, A. Patkos, eds.), JHEP (<http://jhep.sissa.it/>) Proceedings Section, PrHEP-hep2001/021 and references therein.
- [20] C. Glasman in Proceedings of the EPS International Conference on High Energy Physics, Budapest, 2001 (D. Horvath, P. Levai, A. Patkos, eds.), JHEP (<http://jhep.sissa.it/>) Proceedings Section, PrHEP-hep2001/015 and references therein.
- [21] Z. Trócsányi in Proceedings of the EPS International Conference on High Energy Physics, Budapest, 2001 (D. Horvath, P. Levai, A. Patkos, eds.), JHEP (<http://jhep.sissa.it/>) Proceedings Section, PrHEP-hep2001/018 and references therein.

- [22] I. Bertram in Proceedings of the EPS International Conference on High Energy Physics, Budapest, 2001 (D. Horvath, P. Levai, A. Patkos, eds.), JHEP (<http://jhep.sissa.it/>) Proceedings Section, PrHEP-hep2001/014 and references therein.
- [23] The OPAL Collaboration, abs. 202, HEP2001, Budapest.
- [24] V. Andreev in Proceedings of the EPS International Conference on High Energy Physics, Budapest, 2001 (D. Horvath, P. Levai, A. Patkos, eds.), JHEP (<http://jhep.sissa.it/>) Proceedings Section, PrHEP-hep2001/022 and references therein.
- [25] S. Caron in Proceedings of the EPS International Conference on High Energy Physics, Budapest, 2001 (D. Horvath, P. Levai, A. Patkos, eds.), JHEP (<http://jhep.sissa.it/>) Proceedings Section, PrHEP-hep2001/016 and references therein.
- [26] M. Glück, E. Reya and A. Vogt, *Phys. Rev.* **D 45** (1992) 3986.
- [27] S. Frixione in Proceedings of the EPS International Conference on High Energy Physics, Budapest, 2001 (D. Horvath, P. Levai, A. Patkos, eds.), JHEP (<http://jhep.sissa.it/>) Proceedings Section, PrHEP-hep2001/025 and references therein.
- [28] M. Beneke and V. M. Braun, hep-ph0010208.
- [29] Y. L. Dokshitzer and B. Webber, *Phys. Lett.* **B 352** (1995) 451 and references therein.
- [30] G. Grunberg, *Phys. Rev.* **D 29** (1984) 1395.